Rev.Adv.Mater.Sci. 13 (2006) 33-40

FRACTURE OF BULK FACE CENTERED CUBIC (FCC) METALLIC NANOSTRUCTURES

F. Ebrahimi, A. J. Liscano, D. Kong, Q. Zhai and H. Li

Materials Science and Engineering Department, University of Florida, P.O. Box 116400, Gainesville, FL 32611, USA

Received: July 07, 2006

Abstract. Conventional face centered cubic (fcc) metals do not exhibit a ductile-to-brittle transition because spontaneous dislocation emission from the crack tips in these materials inhibits the stresses to be raised high enough for breaking atomic bonds, i.e. brittle fracture. The results of tensile testing of fcc nanolayered and nanocrystalline metals suggest that when the microstructural length scale is reduced to nanoregime cleavage fracture becomes possible in these materials. It is also shown that the stress-state, similar to bcc (body-centered-cubic) metals, affects the fracture behavior considerably. These observations are discussed in terms of the development of internal stresses during the deformation of metallic nanostructures.

1. INTRODUCTION

Plastic deformation of metals, in general, occurs by motion of dislocations. In crystalline materials, plastic deformation is unhomogeneous by nature and takes place on specific slip systems. In conventional large-grained polycrystalline materials (grain size in micrometer range) slip begins preferentially in grains with the highest Schmid factor. The strain incompatibility between elastic and plastic grains increases the local stresses high enough to initiate plastic deformation in elastic grains. For example, the formation of dislocation pile-ups at grain boundaries is one mechanism that results in the development of high internal stresses. With increasing strain, work hardening and crystal rotation make the activation of multiple slip systems possible.

Barriers to dislocation motion increase the metals' strength by requiring the dislocation lines to bow. When the structural scale (e.g., grain size in nanocrystalline and layer thickness in nanolayered materials) is reduced to the nanoregime, high stresses are needed to bow dislocation lines, and therefore strength is increased significantly [1]. Because of the high stress level needed for moving dislocations in nanoregime, small changes in length scale or crystal orientation significantly affect the probability of dislocation motion at a given applied stress level. Consequently, as a result of length scale distribution, even at noticeable applied strain levels, the smaller features remain elastic [2]. The strain incompatibility between the elastic and plastic domains can raise local stresses to high enough levels to cause breaking of atomic bonds, i.e. cleavage [3].

In conventional single-phase metals, the internal stresses developed due to strain incompatibility can cause brittle fracture if (i) the stress required to move dislocations (friction stress) is very high, (ii) recovery of dislocation substructure is difficult, and/or (iii) there is not enough number of slip systems available. For bcc (body centered cubic) metals, reducing temperature significantly increases the friction stress and hence they exhibit a ductile-to-brittle transition with decreasing test temperature. Dislocation cross-slip is limited in low stacking fault energy materials and consequently they are usually prone to shear localization and brittle fracture. Von Mises's has demonstrated that five independent slip systems are required to allow each grain to go through a general change of shape [4]. We have shown that in materials with limited number of slip systems, the strain incompatibility results in brittle intergranular

Corresponding author: F. Ebrahimi, e-mail: febra@mse.ufl.edu

fracture (plasticity-induced intergranular fracture) [5,6].

Recovery processes such as dislocation cross-slip and climb relieve the stress concentrations at dislocation pile-ups or within dislocation cell boundaries in large-grained conventional metals. In nanostructured materials, interfacial or grain boundary related deformation mechanisms, e.g. grain boundary sliding and rotation, become prominent [7-14]. These mechanisms can potentially relax the internal stresses developed due to slip within the grains. For example, annealing of nanocrystalline metals has been shown to reduce tensile elongation significantly in spite of grain growth [15-17]. This behavior has been attributed to the inhibition of grain boundary mediated deformation mechanisms through lowering of the grain boundary energy [18] as well as by possible changes in the angle between adjacent boundaries upon annealing [19]. The retardation of deformation through grain boundaries may reduce the relaxation of internal stresses developed by intragranular deformation and increase the probability of brittle fracture [17]. On the other hand, the difficulty in grain boundary sliding produced by a change in the dihedral angles can also encourage crack formation at triple junctions [19].

In metals, plastic deformation always precedes fracture, even in nanostructured form [20-26]. Stress-state has been known to influence the fracture mode of metals such as steels. As the triaxiality at the crack is decreased the normal stress distribution (perpendicular to the crack plane) in the plastic zone is reduced to lower levels. Consequently, the probability of brittle fracture under plane-stress condition is much less than under plane-strain condition. For this reason, the shear-lips always fracture by microvoid coalecense mechanism.

Conventional face centered cubic (fcc) metals do not exhibit a ductile-to-brittle transition because dislocation activities (generation, motion, recovery, etc.) inhibit the stresses to be raised high enough for breaking atomic bonds, i.e. cleavage. Tensile specimens of very pure single-phase fcc metals usually fracture to a point in a completely ductile manner. Due to strain incompatibility, the presence of second-phase particles allows the stresses to build up at their interfaces with the matrix. These stresses are high enough to cause interfacial decohesion or in the case of brittle particles fracture of them. But due to dislocation activities at the crack tip, the crack can not propagate in the matrix in a brittle manner and hence fracture is achieved by the microvoid coalescence mechanism. However, in nanostructured fcc metals brittle fracture is possible even in single-phase materials. Two factors contribute to the occurrence of cleavage in these materials, namely high stress levels needed for dislocation motion and the unhomogeneity of plastic deformation as described previously. Through detailed analysis of matching fracture surfaces and studying the crack profile we have recently demonstrated that the void-like features observed on the fracture surface of nanocrystalline materials has a cup-cone nature and indeed takes place by breaking atomic bonds [3]. Simulation [27] and experimental [3,28] results have demonstrated that fracture in nanocrystalline fcc metals takes place intergranularly. Theoretical modeling has demonstrated that accumulation of grain boundary dislocations at triple junctions can also account for the nucleation of grain boundary cracks in nanocrystalline metals [29]. Considering that grain boundaries in nanocrystalline metals have similar structure as those in coarse-grained materials, it has been suggested that the lack of multiple slip activation in nanograins also contributes to the development of internal stresses that cause intergranular fracture [26].

The purpose of this paper is to present results regarding the fracture of electrodeposited nanostructured fcc metals in the form of nanolayered and nanocrystalline and elucidate the role of length scale, interfacial structure/composition and stress-state on the probability of brittle fracture in these materials.

2. EXPERIMENTAL PROCEDURES

Two types of microstructure, nanolayered and nanocrystalline, were fabricated using electrodeposition techniques. The details of synthesis of these materials have been reported elsewhere [21,24,30]. Since we did not use any additives in the electrolytic bath, the grain boundaries and interfaces were relatively pristine in the fabricated materials. Typically, the deposits were 30 to 50 μm thick and were grown on a round copper substrate with a 3.5 mm diameter.

After deposition, the discs were cut into four rectangular strips and then the copper substrate was removed chemically. Dog-bone shaped tensile specimens with 5 to 10 mm gage length were prepared from the strips by careful hand grinding. Tensile testing was conducted at a nominal strain rate of $2 \cdot 10^{-4}$ s^{-1} at room temperature using pneumatic grips. At least two tensile specimens per condition were tested.

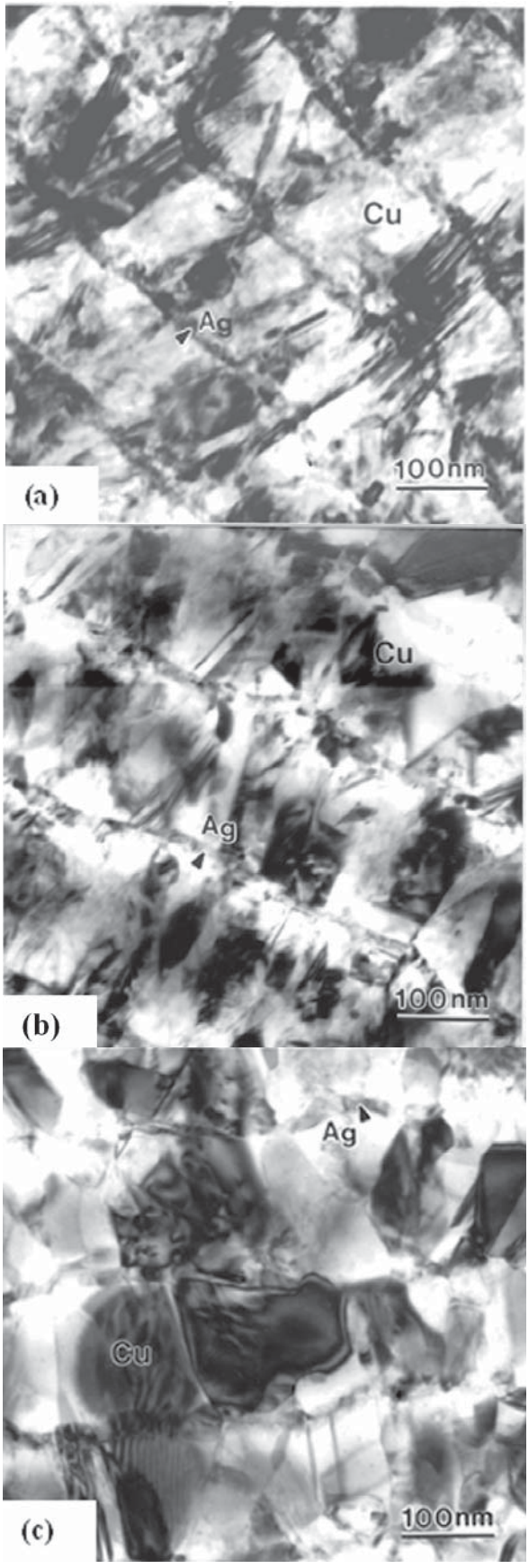

Fig. 1. TEM pictures showing the microstructure of the Cu/Ag laminated samples in (a) as-deposited, (b) annealed at 100 °C and (c) annealed at 150 °C.

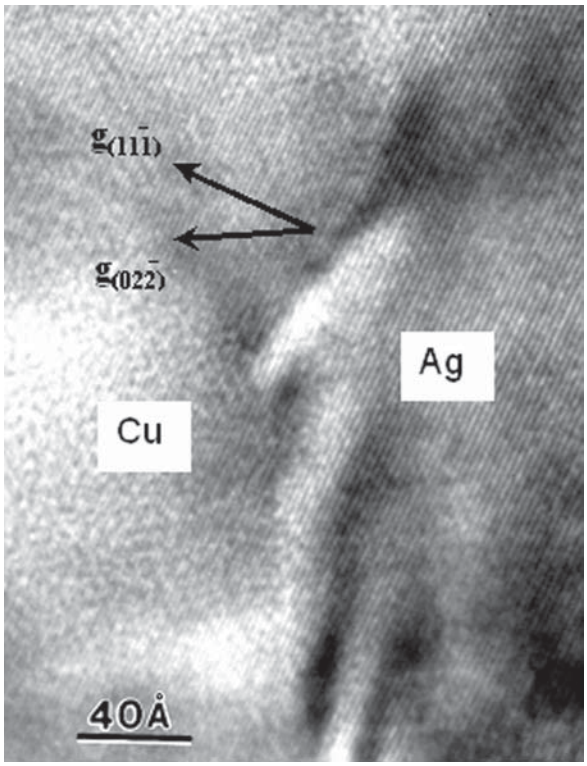

Fig. 2. HRTEM picture imaging the Cu/Ag interface edge-on. Note the continuity of a {111} plane across the layers.

For microstructural evaluation, cross-sectional TEM (transmission electron microscope) samples were prepared from selected deposits using ion milling performed at liquid nitrogen temperature. The fracture surfaces of tensile specimens were studied using SEM (scanning electron microscopy) technique. The composition of the alloys and the multilayered structures were measured using EPMA (electro probe microanalysis) technique.

3. RESULTS AND DISCUSSION

3.1. Copper-silver multilayers – effect of annealing

Copper/silver nanolayered deposits with a bi-layer of λ = 110 nm (λ_{Cu} = 90 nm, λ_{Ag} = 20 nm) were characterized in the as-deposited as well as annealed states (6 hours at 100 °C and 150 °C). Fig. 1 presents the cross-sectional TEM micrographs of these samples. The microstructure of the as-deposited multilayer consisted of nanocrystalline columnar copper grains with extremely fine width (<20

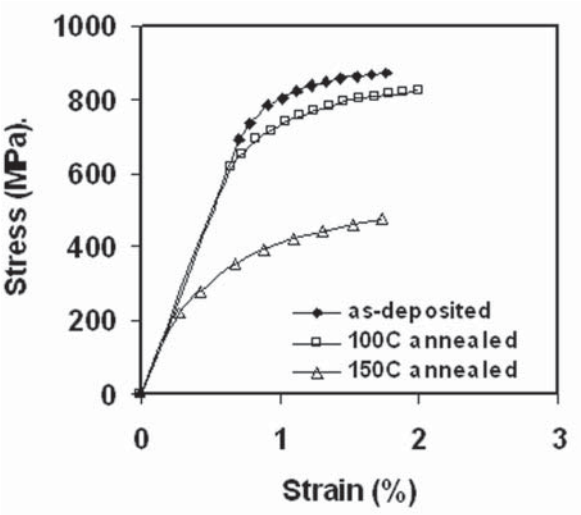

Fig. 3. Tensile stress-strain curves for nanolayered Cu/Ag samples in as-deposited and annealed conditions.

nm) and length equal to the layer thickness. There is an approximately 13% lattice parameter mismatch between copper and silver, and therefore their interface was not straight. Fig. 2 presents a high resolution TEM micrograph demonstrating that copper and silver layers have the same crystal orientation and the interface seems to zig-zag along the {111} and {110} planes. As can be seen in Fig. 1, annealing resulted in an increase in the copper grain size. Since copper and silver have very low solubility in each other no extensive mixing of the atoms at the interfaces upon annealing is expected. However, signs of silver layer spheroidization were found in the 150 °C annealed samples.

Fig. 3 presents typical tensile stress-strain curves for the Cu/Ag multilayered samples. The as-deposited sample exhibited average yield and ultimate tensile strengths of 676 MPa and 826 MPa, respectively, which are over ten times of strength levels for conventional coarse-grained copper and comparable to values for heavily twinned ultrafine-grained copper [31]. Annealing at 100 °C, despite a noticeable increase in the grain size, reduced the strength level slightly. However, the strength was dropped significantly after annealing at 150 °C.

High magnification SEM pictures of the fracture surfaces of the Cu/Ag multilayers tested are given in Fig. 4. As-deposited and 100 °C annealed samples showed very limited area reduction and

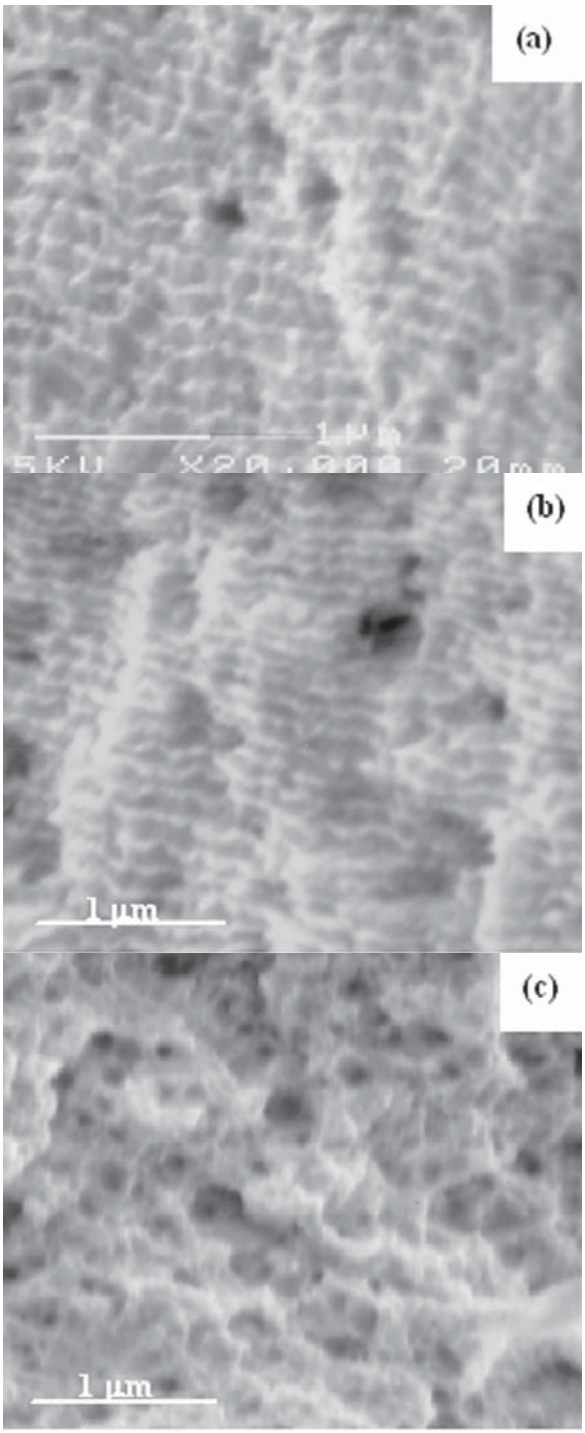

Fig. 4. SEM micrographs showing the fracture surfaces of the Cu/Ag nanolayered samples in (a) as-deposited, (b) annealed at 100 °C and (c) annealed at 150 °C.

fractured in a brittle manner. The layers could be detected easily on the fracture surfaces and no obvious layer delamination was detected (Figs. 4a and

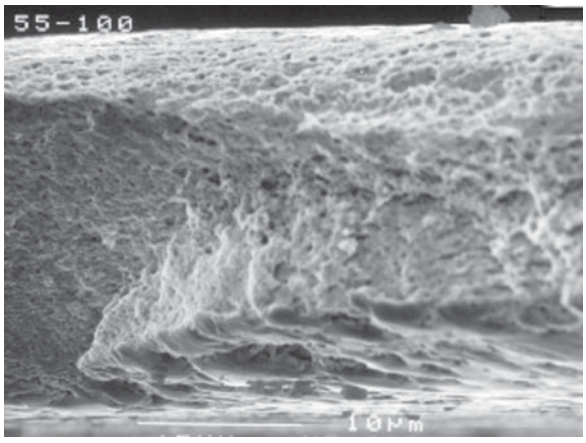

Fig. 5. SEM fractograph showing the drastic increase in the reduction in area as the crack approaches the edge of the 100 °C annealed Cu/Ag nanolayered specimen.

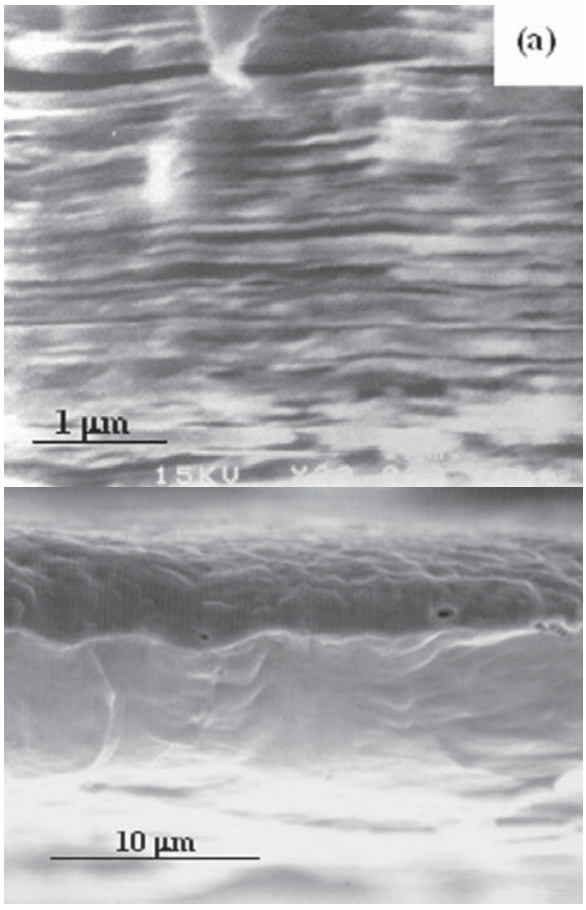

Fig. 6. SEM fractographs showing (a) brittle fracture with extensive delamination in a Ni/Cu nanolayered sample with a bi-layer thickness of 27 nm and (b) completely ductile fracture in a Ni/Cu nanolayered sample with a 6 nm bi-layer thickness.

4b). On the other hand, near the edges of the samples, where the constraint through the width of the sample was lost, extensive necking was observed and fracture resembled a microvoid coalescence mechanism as shown in Fig. 5. The 150 °C annealed sample fractured in a ductile manner as evidenced by the observation of microvoids on the fracture surface (Fig. 4c). For this sample, the layered structure could not be recognized and the sample exhibited considerable reduction in area, suggesting that Cu and Ag layers deformed in a compatible manner.

The above results demonstrate that the Cu/Ag nanolayered samples exhibit a ductile-to-brittle transition with annealing as well as with a change in the stress-state from plane-strain to plane-stress. Both effects modify the development of internal stresses that result from the strain incompatibility between the layers as well as among the nanocrystalline grains in the layers. The very high yield strength of the as-deposited and 100 °C annealed samples along with their continuous silver layer promoted brittle fracture. The significant grain growth and the partial spheroidization of the silver layer after annealing at 150 °C resulted in a 3-fold decrease in yield strength and less opportunity for internal stress accumulation, and hence ductile fracture prevailed.

3.2. Nickel-copper multilayers – effect of layer thickness

In this section the fracture behavior of laminated Ni/Cu multilayers are compared. The lattice parameter of copper and nickel is very close (<3%) and hence their interface can be flat and coherent [32]. However as the layer thickness is increased the interface becomes faceted and incoherent. Fig. 6 compares the fracture behavior of Ni/Cu multilayered tensile specimens with bi-layer thickness values of 27 nm and 6 nm, respectively. The incoherent interfaces in the sample with 27 nm bi-layer thickness make it difficult for dislocations to penetrate [33] and therefore, as shown in Fig. 6a, the fracture mode is brittle. Also, the presence of high level of internal stresses caused interfacial delamination. On the other hand, for the sample with 6 nm bi-layer thickness dislocations can easily traverse the coherent interfaces and as can be seen in Fig. 6b, the sample fractured in a completely ductile manner with the so-called knife-edge behavior.

Similar to the Cu/Ag samples, the stress-state played a role in the level of ductility achieved. Fig. 7 compares the fracture surfaces from the mid-width

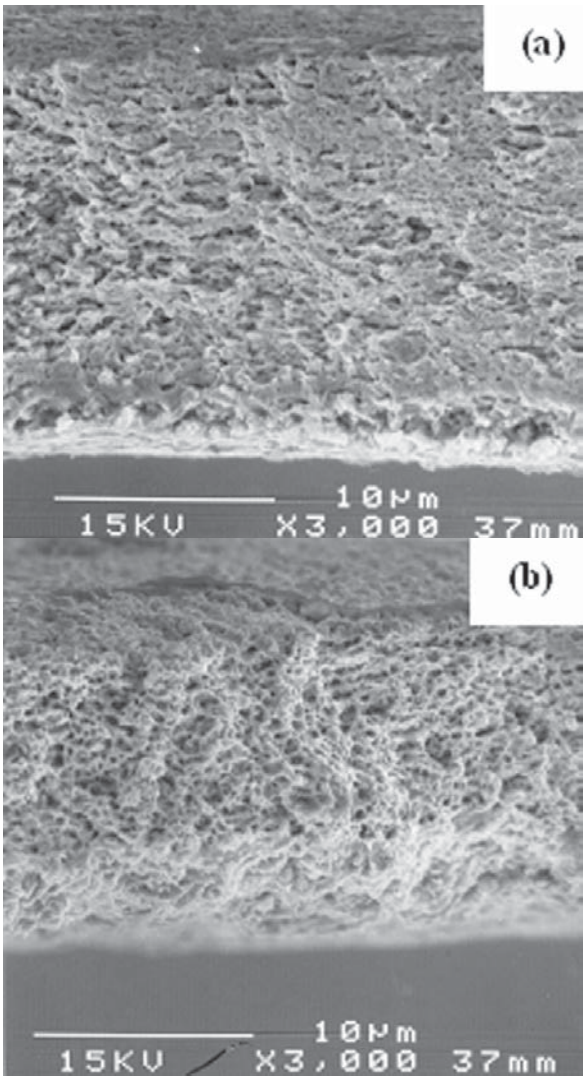

Fig. 7. SEM fractographs showing the change in the degree of area reduction in tensile samples of a Ni/Cu nanolayered sample with a 17.5 nm bi-layer thickness. (a) Mid-section of the sample. (b) Near the edge of the sample.

and near the edge of a sample with a bi-layer thickness of 17.5 nm. Extensive necking can be seen (Fig. 7b) near the edge where the stress-state is closer to a plane-stress condition, while limited reduction in area is found in the mid-section (Fig. 7a).

The above results demonstrate that Ni/Cu nanolayered samples exhibit a ductile-to-brittle transition with a change in the interfacial structure from coherent to incoherent as well as with a change in the stress-state from plane-strain to plane-stress. In comparison to the Cu/Ag nanolayered structure, the interfacial structure had a more pronounced effect in the Ni/Cu structure because of the much finer interlayer spacing and micrometer grain size within the layers.

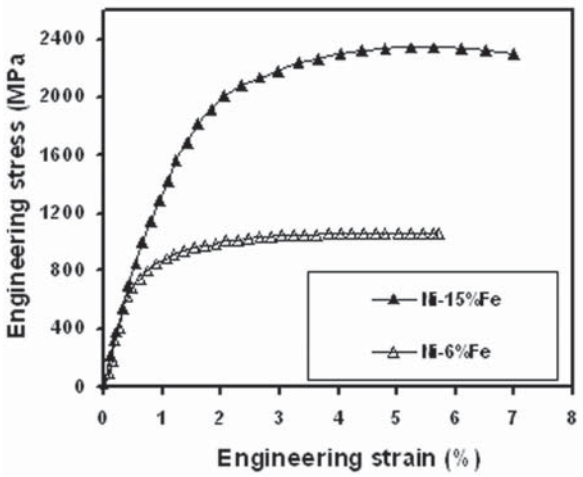

Fig. 8. Tensile stress-strain curves for Ni-Fe alloys with 9 nm (Ni-15%Fe) and 53 nm (Ni-6%Fe) average grain size.

3.3. Single-phase nanocrystalline Ni-Fe alloys – effect of grain size

The stress-strain curve for two Ni-Fe alloys with compositions of 15%Fe and 6%Fe and average grain sizes of 9 nm and 53 nm, respectively, are given in Fig. 8. The alloy with 9nm grain size exhibited much higher yield strength and strain-hardening rate than the alloy with 53 nm grain size [34]. The fracture surfaces of these two alloys are presented in Figs. 9 and 10. The sample with 9nm grain size fractured in a brittle manner in the mid-section (Fig. 9a) and consistent with the multilayered samples more ductility was observed near the edges (Fig. 9b). We have previously demonstrated that cracks nucleate and grow intergranularly in this material [3]. On the other hand, the Ni-6%Fe sample with a 53nm grain size fractured in a completely ductile manner. As shown in Fig. 10a, the sample broke with a knife-edge behavior, but in some areas void nucleation was possible and some microvoids were observed on the fracture surface (Fig. 10b)

Consistent with our previously reported study [25], the above results demonstrate that a change in the grain size in nanocrystalline fcc metals results in a ductile-to-brittle transition. As the grain size is decreased the yield strength is reduced sig-

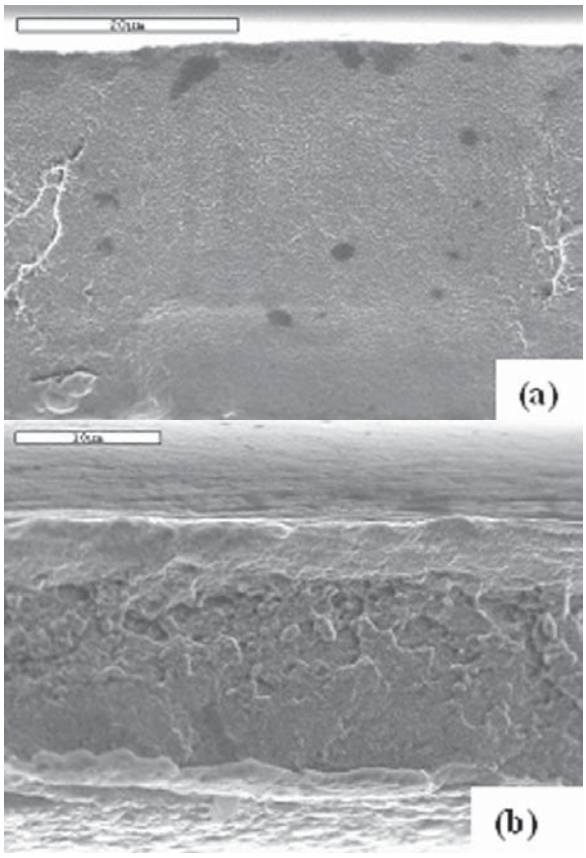

Fig. 9. SEM fractographs of the Ni-15%Fe alloy with an average grain size of 9 nm (a) in mid-section of the sample and (b) near the edge of the sample.

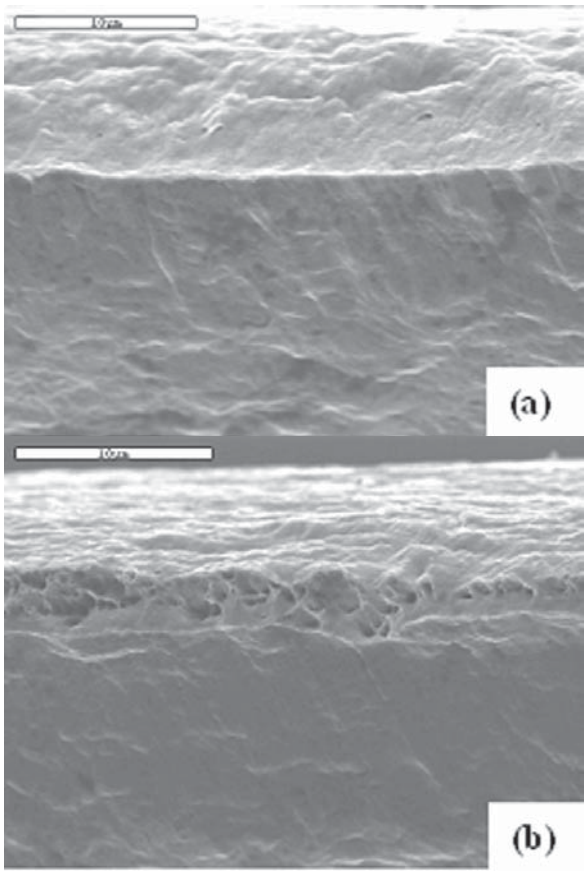

Fig. 10. SEM fractographs showing (a) completely ductile fracture and (b) the presence of some microvoids on the fracture surface of the Ni-6%Fe alloy with an average grain size of 53 nm.

nificantly and the degree of strain incompatibility among grains is diminished, hence resulting in a ductile fracture. Similar to the nanolayered samples, the stress-state also affects the fracture mode by modifying the level of normal stresses achieved in the plastic zone of propagating cracks.

4. CONCLUSIONS

The tensile fracture of electrodeposited Cu/Ag and Ni/Cu multilayers as well as nanocrystalline Ni-Fe alloys was investigated. The results presented in this study leads to the following conclusions:

1. Nanostructured fcc metals can fracture in a brittle manner.
2. Fine grains and continuous incoherent interfaces promote cleavage farcture.
3. Similar to bcc metals, the stress-state affects the fracture behavior.
4. The occurrence of brittle fracture in nanostructured fcc metals is attributed to the difficulty in moving dislocations because of the spatial constraint as well as the development of large internal stresses owing to the strain incompatibility between adjacent layers or grains.

ACKNOWLEDGEMENTS

Financial support for this research has been provided by the National Science Foundation under the grants DMR-9527624, DMR-9980213, and DMR-0605406.

References

[1] J. D. Embury and J. P. Hirth // *Acta Metall. Mater.* **42** (1994) 2051.
[2] F. Ebrahimi, Z. Ahmed and K. L. Morgan // *MRS Proc.* **634** (2001) B2.7.1.

[3] H. Li and F. Ebrahimi // *Adv. Mater.* **17** (2005) 1969.
[4] G. E. Dieter, Mechanical Metallurg. (Third Edition, McGraw-Hill, NY, 1985).
[5] F. Ebrahimi and J. R. Castillo-Gomez // *Acta Metall. Mater.* **40** (1992) 1409.
[6] F. Ebrahimi and G. T. Hoyle // *Acta Mater.* **45** (1997) 4193.
[7] W. W. Milligan, S. A. Hackney, M. Ke and E. C. Aifantis // *Nanostructur. Mater.* **2** (1993) 267.
[8] M. Ke, S. A. Hackney, W. W. Milligan and E. C. Aifantis // *Nanostructur. Mater.* **5** (1995) 689.
[9] H. Hahn and K. A. Padmanabhan// *Phil. Mag.* **76** (1997) 559.
[10] J. Schiřtz, F. D. Di Tolla and K. W. Jacobsen // *Nature* **391** (1998) 561.
[11] H. Van Swygenhoven, M. Spaczer and A. Caro // *Acta Mater.* **47** (1999) 3117.
[12] V. Yamakov, D. Wolf, S. R. Phillpot, A. K. Mukherjee and H. Gleiter // *Philos. Mag. Lett*. **83** (2003) 385.
[13] M. Yu Gutikin, I. A. Ovid'ko and N. V. Skiba // *Acta Mater.***51** (2003) 4059.
[14] Z. Shan, E. A. Stach, J. M. K. Wiezorek, J. A. Knapp, D. M. Follstaedt and S. X. Mao // *Science* **305** (2004) 654.
[15] J. R. Weertman and P. G. Sanders // *Solid State Phenomena* **35-36** (1993) 249.
[16] Y. M. Wang, S. Cheng, Q. M. Wei, E. Ma, T. G. Nieh and A. Hamza // *Scripta Mater*. **51** (2004) 1023.
[17] F. Ebarhimi and H. Li // submitted to *Materials Science*.
[18] A. Hasnaoui, H. Van Swygenhoven and P. M. Derlet // *Acta Mater*. **50** (2002) 3927.
[19] M. Yu. Gutkin and I. A. Ovid'ko // *Phil. Mag. Lett.* **84** (2002) 655.
[20] F. Ebrahimi, Q. Zhai and D. Kong // *Scripta Mater* **39** (1998) 315.
[21] F. Ebrahimi, Q. Zhai and D. Kong // *Mater. Sci. and Eng*. **255** (1998) 20.
[22] F. Ebrahimi, G. R. Bourne, M. S. Kelly and T. E. Matthews // *Nanostruct. Mater.* **11** (1999) 343.
[23] F. Ebrahimi and D. Kong // *Scripta Mate.***40** (1999) 609.
[24] F. Ebrahimi and A. J. Licano // *Mater. Sci. and Eng*. **301** (2001) 23.
[25] H. Q. Li and F. Ebrahimi // *App. Phys. Lett.* **84** (2004) 4037.
[26] H. Li and F. Ebrahimi // *Acta Mater.* **54** (2006) 2877.
[27] D. Farkas, H. Van Swygenhoven and P. M. Derlet // *Phys. Rev. B* **66** (2002) 060101.
[28] K. S. Kumar, S. Suresh, M. F. Chisholm, J. A. Horton and P. Wang // *Acta Mater* **51** (2003) 387.
[29] I. A. Ovi'ko and A. G. Sheinerman // *Acta Mater.* **52** (2004) 1201.
[30] H. Li and F. Ebrahimi // *Mater. Sci. Eng.* **A347** (2003) 93.
[31] Y. F. Shen, L. Lu, Q. H. Lu, Z. H. Jin and K. Lu // *Scripta Mater.* **52** (2005) 989.
[32] F. Ebrahimi, A. J. Liscano, D. Kong and V. Krishnamoorthy // *Phil. Mag.* **83** (2003) 457.
[33] S. I. Rao, P.M. Hazzledine and D. M. Dimiduk // *MRS Proc.***362** (1995) 67.
[34] H. Li, F. Ebrahimi, H. Choo and P. Liaw // *Mater. Sci.,* in press.